Scientific paper

The Magnetic and Colloidal Properties of $CoFe_2O_4$ Nanoparticles Synthesized by Co-precipitation

Sašo Gyergyek,[1,*] Miha Drofenik[1,2] and Darko Makovec[1]

[1] *Department for Materials Synthesis, Jožef Stefan Institute, Jamova 39, SI-1000 Ljubljana, Slovenia*

[2] *Faculty of Chemistry and Chemical Engineering, University of Maribor, Smetanova 17, SI-2000 Maribor, Slovenia*

* *Corresponding author: E-mail: saso.gyergyek@ijs.si*

Received: 20-12-2013

Dedicated to the memory of Prof. Dr. Marija Kosec.

Abstract

Magnetic $CoFe_2O_4$ nanoparticles were synthesized by co-precipitation at 80 °C. This co-precipitation was achieved by the rapid addition of a strong base to an aqueous solution of cations. The investigation of the samples that were quenched at different times after the addition of the base, using transmission electron microscopy (TEM) coupled with energy-dispersive X-ray spectroscopy (EDXS) and X-ray powder diffractometry, revealed the formation of a Co-deficient amorphous phase and $Co(OH)_2$, which rapidly reacted to form small $CoFe_2O_4$ nanoparticles. The nanoparticles grew with the time of aging at elevated temperature. The colloidal suspensions of the nanoparticles were prepared in both an aqueous medium and in a non-polar organic medium, with the adsorption of citric acid and ricinoleic acid on the nanoparticles, respectively. The measurements of the room-temperature magnetization revealed the ferrimagnetic state of the $CoFe_2O_4$ nanoparticles, while their suspensions displayed superparamagnetic behaviour.

Keywords: Cobalt ferrite, nanoparticles, co-precipitation, colloidal suspensions, magnetic properties

1. Introduction

The unique magnetic properties of magnetic nanoparticles, which are dominated by single-domain ferrimagnetism and superparamagnetism, are of great scientific and technological importance.[1,2] Superparamagnetism is a phenomenon associated with the size reduction of the ferri/ferromagnetic material. When the size of the particles is reduced below a certain limit the thermal fluctuations induce a rapid relaxation of the particles' magnetic moments, relative to the time of observation.[1,2] The critical size for the transition to superparamagnetic behaviour at room temperature depends on the magnetocrystalline anisotropy of the material and is 6–8 nm for $CoFe_2O_4$.[3–5] Superparamagnetic nanoparticles show an advantage over the larger ferrimagnetic nanoparticles when colloidal suspensions have to be prepared. The rapid moment relaxation strongly reduces the magnetic dipolar attractions, which would otherwise cause agglomeration. Colloidal suspensions of superparamagnetic nanoparticles are important in various technological[6] and biomedical applications, for example, in MRI imaging, in targeted drug delivery and in cancer treatments using magnetically-mediated hyperthermia.[7–11] While for biomedical applications aqueous suspensions are needed, for the preparation of some complex materials suspensions in organic liquids are applied as a starting material. For example, for the preparation of nanocomposites where the nanoparticles are embedded in a polymer matrix, suspensions of nanoparticles in moderately polar organic liquids such as monomers are needed.[12–14]

In some cases, single-domain ferrimagnetic nanoparticles show an advantage over superparamagnetic nanoparticles. In the case of magnetically induced hyperthermia, ferrimagnetic nanoparticles display larger values of specific power losses due to the hysteresis losess, which are absent in superparamagnetic nanoparticles.[11] Also, in magnetic data storage the critical size where the information can be stored is limited by the superparamagnetic limit.[15]

For some of these applications the soft spinel ferrites, such as magnetite and maghemite, are suitable. Howe-

ver, cobalt ferrite, $CoFe_2O_4$, displays some special magnetic properties that are not characteristic for the spinel ferrites.[16] Due to a high magnetocrystalline anisotropy, as well as large magnetostrictive and magneto-optical coefficients, cobalt ferrite is a promising material for the fabrication of composite multiferroics, high-density magnetic data-storage devices, mediators for magnetic hyperthermia, etc.

The simple co-precipitation and hydrothermal treatments are known to be suitable methods for the synthesis of single-domain ferrimagnetic $CoFe_2O_4$ nanoparticles.[17] Usually, the growth of the nanoparticles during the synthesis is controlled by the addition of fatty acids, for example, with oleic acid.[17] However, the preparation of colloidal suspensions of fatty-acid-coated ferrimagnetic nanoparticles in a non-polar organic medium was shown to be challenging.[17] Ricinoleic acid, which is isostructural with oleic acid (the only difference being the presence of the hydroxyl group at position C_{12} in the C_{18} tail) is known to be more efficient in the colloidal stabilization of nanoparticles in non-polar and even moderately polar organic liquids.[12] Moreover, the hydroxyl groups are effective functional moieties, because they can be acetylated under mild reaction conditions. For example, Lattuada et al.[18] synthesized various polymer brushes on the surfaces of ricinoleic-acid-coated iron-oxide nanoparticles using the atom transfer radical polymerization technique (ATRP). The hydroxyl group was used to covalently bond the ATRP initiator to the surface of the nanoparticles. The hydroxyl groups on the surface of the nanoparticles can also be used to initiate ring-opening polymerization, a useful method for the synthesis of several biodegradable polymers that are potentially useful for biological and biomedical applications.[19,20] Although the ricinoleic acid provides remarkable colloidal stability in nonpolar and moderately polar organic liquids, it is inefficient for the colloidal stabilization of nanoparticles in highly polar organic liquids and aqueous media. In highly polar media, such as water, the electrostatic charge on the nanoparticle surfaces is usually the reason for the repulsion and colloidal stability. The density of the surface charges on the hydrated surfaces of oxides when exposed to aqueous media is usually too low to prevent agglomeration across a wide pH region. The adsorption of a citriate anion on the nanoparticle surfaces strongly increases their negative surface charge.[21] Citric acid is a tricarboxylic hydroxy acid that forms a coordinate bond between the carboxyl groups and the surface cations, leaving at least one carboxylic group non-bonded, pointing radially towards the aqueous medium.[21] The dissociation of this unbonded carboxyl group and the deprotonation of the hydroxyl group are believed to be the reason for the highly negative surface charge across the wide pH range of the citric-acid-adsorbed oxide surfaces.[21]

In this work the kinetics of the formation of $CoFe_2O_4$ nanoparticles during their co-precipitation with and without the presence of ricinoleic fatty acid was studied. We also present the preparation of colloidal suspensions of single-domain ferrimagnetic $CoFe_2O_4$ nanoparticles and a qualitative description of their colloidal stability in an aqueous and non-polar organic medium. In addition, the role of the presence of the ricinoleic acid during the co-precipitation of the nanoparticles on their size was investigated.

2. Experimental

2. 1. Materials

Cobalt (II) sulphate heptahydrate ($CoSO_4 \cdot H_2O$, Alfa Aesar, 98%), iron (III) sulphate hydrate ($Fe_2(SO_4)_3 \cdot x\text{-}H_2O$, Alfa Aesar, 99+%), sodium hydroxide (NaOH, Alfa Aesar, 98%), nitric acid (HNO_3, AppliChem, 65% p.a.), ricinoleic acid ($C_{18}H_{34}O_3$, TCI, >80%), citric acid ($C_6H_8O_7$, Alfa Aesar, 99+%), acetone (C_3H_6O, AppliChem, p.a.), methanol (CH_4O, Merck, for analysis), toluene (C_7H_8, Merck, for synthesis), were used as received, without further purification. From the corresponding sulphates, stock aqueous solutions of Co^{2+} and Fe^{3+} were prepared (0.584 mol/l and 0.505 mol/l, respectively), and from citric acid, a stock aqueous solution was prepared (2.6 mol/l).

2. 2. Synthesis

The $CoFe_2O_4$ nanoparticles were synthesized according to a previously published method, with some modifications.[17] In brief, 40 ml of an aqueous solution of cations (Co^{2+} 0.175 mol/l and Fe^{3+} 0.354 mol/l) was heated to 80 °C in a three-neck round-bottom flask and 20 ml of NaOH (3.5 mol/l) aqueous solution was added in a single, rapid pour during vigorous stirring. The pH of the suspension after co-precipitation was 13. After aging for 2 hours at 80 °C under reflux, the suspension of precipitates was left to cool naturally to room temperature. The nanoparticles were then washed three times with DDI water to remove the unreacted ions. Finally, the $CoFe_2O_4$ nanoparticles were oven dried at 60 °C and grinded in an agate mortar (CF-NPs).

To obtain the hydrophilic $CoFe_2O_4$ nanoparticles with charged surfaces, citric acid was adsorbed onto the synthesized nanoparticles using the process described previously.[22] In brief, washed $CoFe_2O_4$ nanoparticles were dispersed in DDI water in a round-bottom flask and an aqueous solution of citric acid was (0.6g/ml) was added. The pH value of the suspension was adjusted to the value of pH = 5.2 with the addition of an NH_4OH aqueous solution. The suspension was heated to 80 °C and aged for 1.5 hours. After ageing, the suspension was left to cool naturally to room temperature. The citric-acid-adsorbed $CoFe_2O_4$ nanoparticles were flocculated by the addition of acetone and separated with a permanent magnet. The excess of citric acid was washed out with acetone. The sus-

pension of citric-acid-adsorbed $CoFe_2O_4$ nanoparticles was prepared by dispersing the washed nanoparticles in pure DDI water. To remove any agglomerates the suspension was centrifuged at a relative centrifugal force (RCF) of ~3200 g for 5 minutes (Eppendorf 5804™ centrifuge with F34-6-8 rotor). The suspensions were considered to be stable colloidal suspensions of nanoparticles (CF-CA-S). The citric-acid-adsorbed $CoFe_2O_4$ nanoparticles were isolated from the colloidal suspension CF-CA-S. The nanoparticles were then flocculated by the addition of acetone and separated with a permanent magnet. Finally, the nanoparticles were oven dried at 60 °C and grinded in an agate mortar (sample CF-CA-NPs).

To obtain the hydrophobic $CoFe_2O_4$ nanoparticles, ricinoleic acid was adsorbed onto the synthesized nanoparticles using the process described previously.[12] In brief, after aging the suspension of precipitate for 2 hours at 80 °C under reflux (see the first paragraph for the synthesis of the CF-NPs) 1 g of ricinoleic acid was added in small amounts over a period of 30 min. After cooling to room temperature, diluted HNO_3 was added to decrease the pH to a value of approximately 5. The decrease in the pH value resulted in the flocculation of the hydrophobized $CoFe_2O_4$ nanoparticles. To remove any unreacted ions and excess ricinoleic acid the precipitate was washed three times with DDI water, with acetone and three times with methanol. The suspension of ricinoleic-acid-adsorbed $CoFe_2O_4$ nanoparticles was prepared by dispersing the washed hydrophobic nanoparticles in toluene. To remove any agglomerates the suspension was centrifuged at a relative centrifugal force (RCF) of ~3200 g for 5 minutes (Eppendorf 5804™ centrifuge with F34-6-8 rotor). The suspensions were considered to be stable colloidal suspensions of the nanoparticles (suspension CF-RA-S). The nanoparticles that sedimented during the centrifugation were washed with acetone, oven dried at 60 °C, and grinded in an agate mortar (sample CF-RA-ND-NPs). The nanoparticles were also isolated from the colloidal suspension CF-RA-S, flocculated by the addition of acetone and then separated with a permanent magnet. Finally, the nanoparticles were washed several times with acetone, oven dried, and grinded in an agate mortar (sample CF-RA-D-NPs).

2. 3. Characterization

The phase purity was checked with X-ray powder diffraction (XRD) (Siemens D5000). The crystallite size (d_{XRD}) was estimated from the XRD line broadening using the Scherrer equation.[23] The whole-powder-pattern fitting procedure was employed, where the crystallite size was the fitted parameter using the crystallographic software package Topas™. The contribution of the instrumental broadening of the diffraction lines was described by the convolution of the individual instrumental broadening functions constructed from the instrument parameters.[24] For the TEM investigations a drop of the suspension was dried on a copper-grid-supported, transparent, carbon foil. The transmission electron microscopy (TEM) was performed using a thermionic electron-source TEM JEOL 2100 operated at 200 kV. The particle composition was characterized using energy-dispersive X-ray spectroscopy (EDX) coupled to the TEM. Semi-quantitative analyses were performed using an EDX microanalysis system (Jeol JED-2300) and Jeol Analysis software. The room-temperature magnetization M as a function of the magnetic field H of the samples was measured using a Lake Shore 7307 VSM vibrating-sample magnetometer. The content of inorganic phase ($CoFe_2O_4$) in the samples was determined using thermogravimetry. The dried samples were weighted in corundum crucibles and heated to 500 °C in a laboratory furnace (Nabertherm). After cooling to the room temperature the crucibles were weighted again and the content of inorganic phase was calculated. The hydrodynamic size distributions of the particles in the suspensions were measured using a dynamic light scattering (DLS) Fritsch Analysette 12 DynaSizer. The design of the apparatus enables measurements in a thin film of the suspension, which significantly reduces the probability of multiple scattering of the detected light and thus enables measurements in relatively concentrated, as-prepared suspensions. The ξ-potential of the citric-acid-adsorbed nanoparticles in aqueous media at pH = 7 was measured using a Brookhaven Instruments Corp., ZetaPALS.

3. Results and Discussion

3. 1. Mechanism of Formation

The $CoFe_2O_4$ nanoparticles were synthesized with the co-precipitation of Co^{2+} and Fe^{3+} cations by the addition of a strong base. The precipitations of Co^{2+} and Fe^{3+} cations proceed at markedly different pH values.[17] The precipitation of the Fe^{3+} cations proceeds at a low pH value, in the range between 2.5 and 3.0, whereas the $Co(OH)_2$ precipitates at a much higher pH value of 8.0.[17] The fast addition of the base and the vigorous stirring ensure that a pH value high enough for the simultaneous precipitation of both cations is achieved. It was shown that for similar experimental conditions to those described here (the same concentration and final pH value), that despite the markedly different hydrolytic behaviour of both cations the single-phase stoichiometric $CoFe_2O_4$ nanoparticles are formed at 40 °C.[17] However, the synthesized nanoparticles were of an average diameter of ≈2 nm and therefore exhibited poor magnetic properties.[17] It was also shown that the presence of the surfactant, such as oleic or ricinoleic acid during the co-precipitation, strongly modifies the formation of the spinel phase.[17] The lowest temperature for the formation of the stoichiometric $CoFe_2O_4$ increased to 80 °C.[17] To obtain a better insight into the mechanism of formation the magnetization measured at a magnetic field strength of H = 1 T and the coercivity of

the samples taken at different time intervals after the addition of the base at 80 °C were measured. At specified time intervals after the co-precipitation the sample was taken from the reaction vessel and poured into a large amount of acetone. Because the samples were rapidly cooled to room temperature and because the solubility of the Co and Fe species is practically zero in acetone we believe that all the reactions were quenched. To study the influence of the presence of the ricinoleic acid on the formation of the spinel the same experiment was conducted in the presence of ricinoleic acid during the co-precipitation. The magnetization and coercivity of both samples increased approximately linearly with time up to 30 min after the addition of the base (Figure 1). The rate of increase of the magnetization and coercivity in the time interval between 30 min and 120 min progressively decreased. After 120 min the values of the magnetization and coercivity remained constant. The increase of magnetization and coercivity was higher in the period from 0 to 60 min after co-precipitation for the sample co-precipitated in the absence of ricinoleic acid.

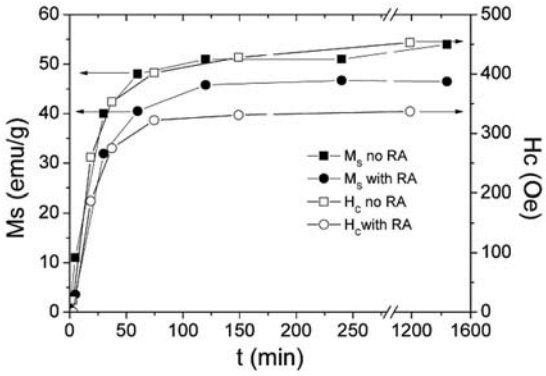

Figure 1. The variation of the magnetization (full symbols) and coercivity (crossed symbols) with time after the addition of NaOH to the solution of the Co^{2+} and Fe^{3+} cations in the absence (square symbols) and in the presence of the ricinoleic acid (round symbols).

The magnetization and coercivity of the sample co-precipitated in the presence of the ricinoleic acid are lower than for the sample synthesized in its absence, indicating a smaller average size. It is worth noting that magnetization not only strongly depends on the average size of the magnetic nanoparticles but also on the content of magnetic material in the sample. Normally, thermogravimetry is used to determine the amount of magnetic material, especially in the samples that also contain organic material, such as ricinoleic acid. The use of thermogravimetry to determine the content of the magnetic material in the samples taken immediately after the co-precipitation would introduce a large error. It is reasonable to believe that the samples taken immediately after co-precipitation also contain hydroxides and oxyhydroxides that would transform to oxides during heating to the temperature of 380 °C needed to decompose the ricinoleic acid.[13] The release of water due to dehydration of the oxyhydroxides would in addition to decomposition of the ricinoleic acid contribute to the weight loos. The coercivity is, in principle, independent of the content of magnetic material in the sample. The significantly lower coercivity of the sample synthesized in the presence of the ricinoleic acid further indicates that the coated nanoparticles are smaller than the nanoparticles synthesized in the absence of ricinoleic acid. The XRD powder patterns were only collected for the samples co-precipitated in the absence of ricinoleic acid. The XRD pattern of the sample taken immediately after the co-precipitation consists only of a broad maxima, indicating its amorphous nature (Figure 2 (a)). However, the reflections characteristic for the cubic spinel phase became clearly visible in the sample taken 5 min after the co-precipitation and became narrower with ageing (Figure 2a). The average size of the nanoparticles increased from ~3 nm at 5 min after the co-precipitation to ~14 nm at 120 min and remained practically constant after 120 min (Figure 2 (b)). The evolution of the average size with time is very similar to the evolution of the magnetization (Figure 1). The average size of the nanoparticles co-precipitated in the presence of the ricinoleic acid at 80 °C and aged for 2 hours estimated from the XRD powder pattern was 7 nm.[17]

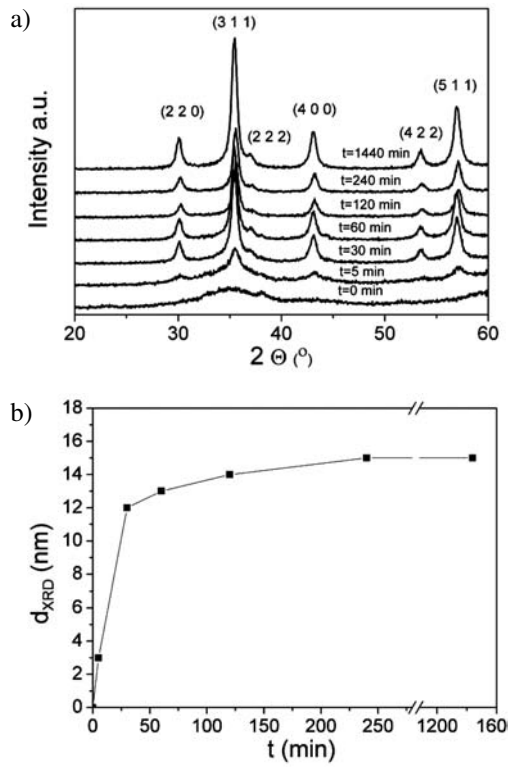

Figure 2. XRD powder patterns of the samples taken at different time intervals after co-precipitation in the absence of ricinoleic acid at 80 °C (a). The variation of the average size of the spinel phase at the same time intervals (b).

The samples taken immediately, 5 min and 30 min after the co-precipitation were also observed on the TEM (Figure 3). The analysis revealed that the sample taken immediately after the co-precipitation was composed of very small, amorphous particles of a Co-deficient composition (Figure 3 (a)). In the same sample, long and thin needle-like particles were also present. The needle-like particles were most likely $Co(OH)_2$, since the EDS analysis showed predominantly Co.

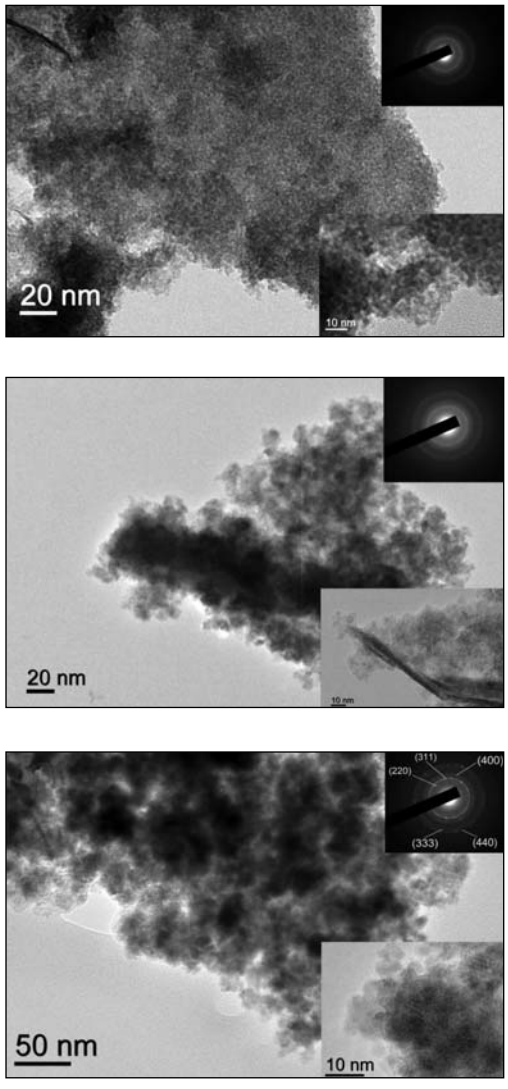

Figure 3. TEM images of the samples taken immediately (a), 5 min (b) and 30 min (c) after the co-precipitation. The insets are the selected-area electron diffraction patterns (SAED) and images acquired at higher magnification. The SAED pattern in Fig 3 (c) was indexed according to the cubic spinel structure.

The sample taken 5 min after the addition of the base is composed of slightly larger crystalline nanoparticles with a more defined shape and nearly stoichiometric composition. The needle-like $Co(OH)_2$ particles are still present (Figure 3 (b)). The sample taken 30 min after the addition of the base is composed only of crystalline nanoparticles of a size in the range between 4 nm to 12 nm, and of the stoichiometric $CoFe_2O_4$ composition (Figure 3 (c)).

From the experimental observations described above a mechanism of formation can be proposed. The addition of the base results in the rapid precipitation of amorphous Co and Fe oxy/hydroxides that react to form very small spinel nanoparticles. The reaction at 80 °C is relatively fast since only 5 min after the co-precipitation the reflections characteristic for spinel are present and no broad maxima characteristic for the amorphous phase are present. The evident growth of the spinel phase (Figure 1 and 2) is most likely a result of the Ostwald ripening process. The process is caused by the solubility difference between larger and smaller particles, which are more soluble, as described by the Gibbs-Thomson equation.[25] The slower growth resulting in the smaller average size of the spinel nanoparticles co-precipitated in the presence of the ricinoleic acid is also related to the Gibbs-Thomson relation. It is well known that fatty acids, such as ricinoleic acid, form a bilayer structure on the oxide nanoparticles in aqueous media.[26] The $–COO^-$ groups of the ricinoleic acid form a coordinate bond with the surface cations of the oxide phase and form a first layer. Because the ricinoleic acid is present in a much larger amount to form a monolayer, the hydrophobic tails of the second layer associate in such a way that their $–COO^-$ groups direct towards the aqueous media. Because of the bilayer the surface tension of the nanoparticles is strongly reduced from approximately 55 mJ/m^2, which is a typical value for the spinel phase,[27] to a value in the range between 10 mJ/m^2 and 20 mJ/m^2, typical for micellar solutions of surfactants bearing $–COO^-$ groups.[28] According to the Gibbs-Thomson equation, a solid exhibiting a lower surface tension is also less soluble.[25] The nanoparticles co-precipitated in the presence of the ricinoleic acid display a lower solubility with respect to the nanoparticles co-precipitated in the absence of the acid. Therefore, the driving force for their growth is lower, which results in their slower growth and smaller average size.

3. 2. $CoFe_2O_4$ Nanoparticles

The magnetic and colloidal properties of $CoFe_2O_4$ nanoparticles in aqueous and organic non-polar media are of great importance for their applications in various fields. The $CoFe_2O_4$ nanoparticles were synthesized by the co-precipitation of Co^{2+} and Fe^{3+} cations with the addition of a strong base at 80 °C. The suspension was aged for 2 hours at 80 °C. As shown above, the particles' growth ceases after this period. To prepare colloidal suspensions in aqueous media and non-polar organic media the nanoparticles' surfaces were modified by bonding citric or ricino-

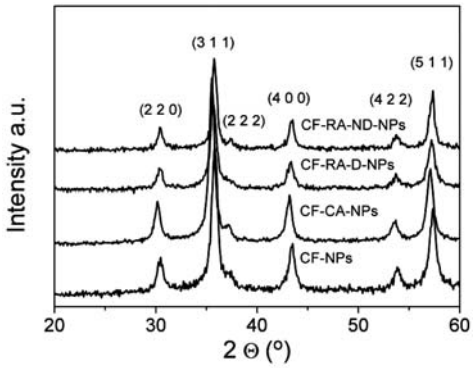

Figure 4. XRD patterns of the synthesized nanoparticles.

leic acid, respectively. The surface modification was conducted post synthesis to ensure comparable size distributions of the modified nanoparticles, since the presence of a surfactant clearly modifies the growth of the nanoparticles.

The XRD pattern of the nanoparticles CF-NPs is composed only of broad reflections characteristic for the spinel structure (Figure 4). The average size estimated from the broadening of the XRD reflections was found to be 14 nm. The nanoparticles CF-NPs strongly agglomerated during drying on the supporting film of the TEM specimen grid (Figure 5 a). Because of the agglomeration a precise measurement of the size of an individual nanoparticle was not possible and therefore the estimation of the size distribution function is not feasible. However, an estimation on the size can be made. Clearly, the size distribution is broad: the particle sizes ranges from 5 nm to 20 nm (Figure 5 (a)).

The nanoparticles CF-NPs exhibit ferrimagnetic behaviour at room temperature (Figure 6 (a) and Table 1). However, the magnetization of the nanoparticles does not reach saturation at the maximum applied field of 1 T, because of their small size.[1] The magnetic nanoparticles have a structurally and magnetically disordered surface layer, which cannot reach saturation in magnetic fields that are achievable with conventional magnetometers. However, the slope of the magnetization is rather low at high fields and the magnetization obtained at a field strength of 1 T is a reasonably good estimation of the saturation magnetization (Figure 6). The magnetizations of the nanoparticles are lower than the saturation magnetization of the bulk $CoFe_2O_4$ (80 emu/g)[16] because of their small size.[1]

Table 1. Size and room-temperature magnetic properties of nanoparticles.

Sample name	d_{XRD} (nm)	M (emu/g)[a]	Hc (Oe)
CF-NPs	14	57.0	563
CF-CA-NPs	15	61.0	567
CF-RA-D-NPs	13	60.0	441
CF-RA-ND-NPs	19	63	1277

[a] Magnetization at field strength H=1T. The value is normalized per g of $CoFe_2O_4$.

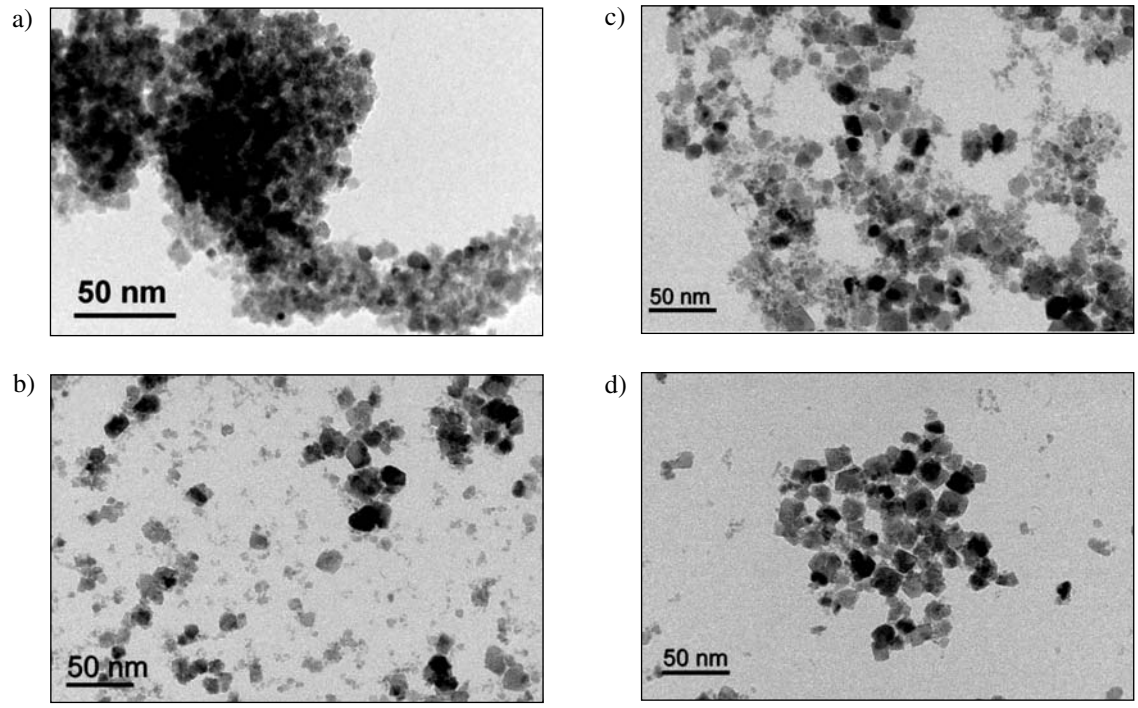

Figure 5. TEM images of the nanoparticles CF-NPs (a), CF-CA-NPs (b), CF-RA-D-NPs (c) and CF-RA-ND-NPs (d).

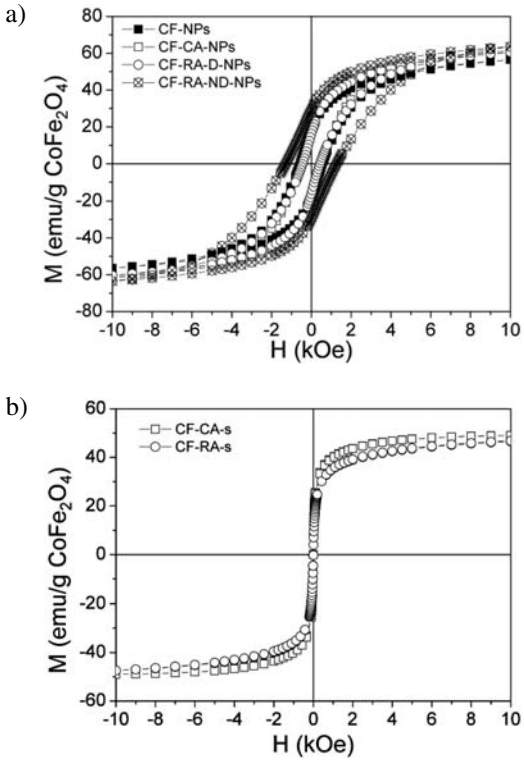

Figure 6. Room-temperature magnetization curves of the nanoparticles (a) and suspensions prepared from the nanoparticles (b).

3. 2. Colloidal Suspension of $CoFe_2O_4$ Nanoparticles

The colloidal behaviours of the aqueous and non-polar organic suspensions of the $CoFe_2O_4$ nanoparticles were studied. A profound difference in the colloidal stability between the aqueous and organic suspensions was first noted in the centrifugation step of the suspensions' preparation. When the suspension of citric-acid-coated nanoparticles was centrifuged, all of the nanoparticles remained dispersed in the liquid. On the other hand, a relatively large amount of nanoparticles separated from the suspension of the ricinoleic-acid-coated nanoparticles in toluene. The average size of the separated fraction CF-RA-ND-NPs was estimated from XRD reflection broadening and was found to be 19 nm, which is larger than the average size of the nanoparticles CF-NPs (Table 1). The large average size of the nanoparticles CF-RA-ND-NPs is also evident from the relatively large coercivity displayed by the nanoparticles (Table 1). The nanoparticles CF-RA-D-NPs that were isolated from the colloidal suspension were smaller than the nanoparticles CF-NPs and displayed a lower coercivity (Table 1). The difference in the nanoparticle sizes is not clearly evident from the TEM images, because the nanoparticles strongly aggregated during the drying on the support film of the TEM specimen grid (Figure 5). The observed separation is most likely caused by the strong magnetic attraction between the nanoparticles larger than approximately 15 nm, which is not counter balanced by the repulsion between the ricinoleic acid chains of the approaching nanoparticles. The nanoparticles that were dispersed in both the aqueous and the organic media are ferrimagnetic at room temperature (Figure 6 (a) and Table 1), while the suspensions displayed typical superparamagnetic behaviour, showing no remanence and coercivity (Figure 6 (b)). In colloidal suspensions the nanoparticles are also subjected to rotational motion in addition to Brownian movement.[29] The rotation of the individual nanoparticles is the reason for the randomization of the magnetic moments in the absence of an external magnetic field and consequently for the superparamagnetic behaviour. It is worth noting that the individual nanoparticles are still in the ferrimagnetic state, although their suspensions show superparamagnetic behaviour because of the moment relaxation with the rotational motion. However, the frequency of such rotations is inversely proportional to the size of the nanoparticles.[29] The probability that the two approaching nanoparticles are oriented in such a way that the magnetic dipolar interaction is attractive is therefore inversely proportional to the size of the nanoparticle. This means that even if the colloidal suspension displays superparamagnetic behaviour there will be a larger number of events that would result in agglomeration if the magnetic and van der Waals attractions are not prevented. The variation of the diffusion coefficient or the hydro/solvodynamic diameter of the nanoparticles dispersed in a liquid medium on their concentration can give an insight into whether the colloidal system is attractive or repulsive.[30] The hydrodynamic diameter of the nanoparticles CF-CA-NPs was estimated to be 22 nm and 47 nm at a concentration of 1.8 g/l and at infinite dilution, respectively. The increase in the hydrodynamic size with a decrease of the concentration of nanoparticles indicates that the system is repulsive.[30] The repulsion is expected because the measured ξ-potential of the nanoparticles CF-CA-NPs at the same neutral pH as the measurements of the hydrodynamic diameter and the magnetic properties of the suspension CF-CA-s was found to be strongly negative (–40 mV). The solvodynamic diameter of the nanoparticles CF-RA-D-NPs was estimated to be 44 nm and 41 nm at concentrations of 19.0 g/l and at infinite dilution, respectively. The slight decrease indicates that the system is attractive.[30] A similar system of magnetic nanoparticles stabilized in a non-polar organic medium by the adsorption of unsaturated fatty acid, such as ricinoleic acid, was also found to be attractive and at the same time colloidal.[12] A qualitative difference in the description of the interaction energy between two particles dispersed in aqueous or organic media obviously exists. In the aqueous media the energy barrier is clearly high enough to prevent agglomeration, even of the largest citric-acid-coated nanoparticles of ~ 20 nm in size that are present in the sample. The reason is the highly negative surface charge. In contrast, in the organic media the at-

traction between the nanoparticles larger than ~15 nm in size is high enough to cause their agglomeration.

4. Conclusions

The co-precipitation of $CoFe_2O_4$ nanoparticles at 80 °C was studied. The addition of a strong base to an aqueous solution of cations results in the precipitation of an amorphous Co-deficient phase and $Co(OH)_2$. The precipitates react to form very small $CoFe_2O_4$ nanoparticles, which at a later stage grow through the Ostwald ripening process, reaching a final size of ~14 nm. The ricinoleic acid, which adsorbs on the formed nanoparticles, inhibits their growth. The adsorption of the ricinoleic acid reduces the nanoparticles' solubility, thus decreasing the driving force for the Ostwald ripening.

The $CoFe_2O_4$ nanoparticles were synthesized using the co-precipitation of the Co^{2+}/Fe^{3+} aqueous solution at 80 °C. The synthesized ferrimagnetic nanoparticles displayed a saturation magnetization and coercivity of 57 emu/g and 563 Oe, respectively. The adsorption of the citrate anion on the nanoparticle surfaces enabled the preparation of the aqueous colloidal suspension. The adsorption of ricinoleic acid on the nanoparticle surfaces enabled the preparation of the colloidal suspension in toluene. However, the ricinoleic acid was not efficient in preventing the agglomeration of nanoparticles larger than ~15 nm in toluene due to the attractive magnetic interactions. Both suspensions displayed superparamagnetic behaviour, despite the ferrimagnetic nature of the dispersed nanoparticles.

5. Acknowledgments

The support by the Ministry of Higher Education, Science and Technology of the Republic of Slovenia within the National Research Program P2-0089 is gratefully acknowledged. The authors also acknowledge the use of equipment in the Centre of Excellence on Nanoscience and Nanotechnology – Nanocenter.

6. References

1. R. H. Kodama, *J Mag Mag Mater* **1999,** *200,* 359–372.
2. X. Batlle, A. Labarta, *J Phys D: Appl Phys* **2002**, *35*, R15-R42.
3. R. D. Desautels, J. M. Cadogan, L. van Lierop, *J Appl Phys* **2009,** *105*, 07B506.
4. C. Vázquez- Vázquez, M. Lovelle, C. Mateo, M. A. López-Quintela, M. C. Buján-Núnez, D. Serantes, D. Bladomir, J. Rivos, *Phys Stat Sol (a)* **2008,** *205*, 1358.
5. G. Baldi, D. Bonacchi, C. Innocenti, G. Lorenzi, C. Sangregorio, *J Mag Mag Mater* **2007,** *311*, 10.
6. S. Odenbach, *J Phys: Cond. Matter* **2004**, *16*, R1135.
7. Q. A. Pankhurst, J. Conolly, S.K. Jones, J. Dobson, *J Phys D:Appl Phys* **2003**, *36*, R167-R181.
8. U. Häfeli, W. Schüt, J. Teller, M. Zborowski, Scientific and Clinical Applications of Magnetic Carriers, Plenum, New York, **1997**.
9. M. Arruebo, R. Fernández-Pacheco, M. R. Ibarra, J. Santamaría, *Nano Today* **2007**, *2,* 22–32.
10. M. Veverka, P. Veverka, O. Kaman, A. Lancok, K. Zaveta, E. Pollert, K. Knizek, J. Bohacek, M. Benes, P. Kaspar, E. Duguet, S. Vasseur, *Nanotechnology* **2007**, *18,* 345704 1–7.
11. E. Kita, T. Oda, T. Kayano, S. Sato, M. Minagawa, H. Yanaghira, M. Kishimoto, C. Mitsumata, S. Hashimoto, K. Yamada, N. Ohkohchi, *J. Phys. D:Appl. Phys*. **2010**, *43,* 474011.
12. S. Gyergyek, D. Makovec, M. Drofenik, *J Colloid Interface Sci*. **2011**, *354*, 498–505.
13. S. Gyergyek, D. Makovec, M. Huskić, M. Drofenik, *Colloids Surf. A: Physicochem. Eng. Aspects* **2008**, *317*, 49–55.
14. S. Gyergyek, D. Makovec, A. Mertelj, M. Huskić, M. Drofenik, *Colloids Surf. A: Physicochem. Eng. Aspects* **2010**, *366*, 113–119.
15. A. Moser, K. Takano, D. T. Margulies, M. Albrecht, Y. Sonobe, Y. Ikeda, S. Sun, E. E. Fullerton, *J. Phys. D.:Appl. Phys*. **2002**, *35*, R157-R167.
16. J. Smit, H. P. J. Wijn, Ferrites, Philips' Technical Library, Eindhoven, The Netherlands, **1959**.
17. S. Gyergyek, M. Drofenik, D. Makovec, *Mater Chem Phys* **2012**, *133*, 515–522.
18. M. Lattuada, T. A. Hatton, *Langmuir*, **2007**, *23,* 2158–2168.
19. I. S. Choi, R. Langer, *Macromolecules* **2001**, *34*, 5361–5363.
20. A. M. Schmidt, *Macromol. Rapid. Commun*. **2005**, *26*, 93.
21. P. C. Hidber, T. J. Graule, L. J. Gaukler, *J Am Ceram Soc* **1996**, *79*, 1857–1867.
22. S. Campelj, D, Makovec, M. Drofenik *J Phys: Condens Mat* **2008**, *20*, 1–5.
23. B. D. Cullity, Elements of X-ray Diffraction, Addison-Wesley, Reading, UK, **1987**.
24. R. W. Cheary, A. Coelho, *J Appl Cryst* **1992**, *25*, 109–121.
25. T. Sugimoto, Mondispersed Particles, Elsevier, Amsterdam, The Netherlands, **2001.**
26. L. Shen, P. E. Laibinis, T. A. Hatton, *Langmuir* **1999**, *15*, 447–453.
27. C. Galindo-González, J. de Vicente, M. M. Ramos-Tejada, M. T. López- López, F. Galindo-Caballero, J. D. G. Durán, *Langmuir* 2005, *21*, 4410.
28. M. Malmsten, Surfactants and Polymers in Drug Delivery, Marcel Dekker, New York, USA, **2002.**
29. W. F. Brown, *J Appl Phys* **1963**, *34*, 1319.
30. A. Mertelj, L. Cmok, M. Čopič, *Phys Rev E* **2009**, *79*, 041–402.

Povzetek

Magnetne nanodelce $CoFe_2O_4$ smo sintetizirali s soobarjanjem na temperaturi 80 °C. Soobarjanje smo dosegli s hitrim dodatkom močne baze k vodni raztopini kationov. Mehanizem nastanka nanodelcev $CoFe_2O_4$ smo študirali tako, da smo odvzeli vzorce pri različnih časovnih intervalih po dodatku baze in ustavili kemijske reakcije. Analize vzorcev s presevno elektronsko mikroskopijo (TEM) v kombinaciji z EDXS spektroskopijo in rentgensko praškovno difrakcijo (XRD) so pokazale nastanek amorfne Co deficitne faze in $Co(OH)_2$, ki hitro reagirata in nastanejo majhni $CoFe_2O_4$ nanodelci. Med staranjem na povišani temperaturi nanodelci rastejo. Koloidne suspenzije nanodelcev v vodnem in organskem nepolarnem mediju smo pripravili z adsorpcijo citronske ozirom ricinolejske kisline. Meritve magnetnih lastnosti na sobni temperaturi so pokazale ferimagnetne lastnosti nanodelcev $CoFe_2O_4$ medtem, ko so suspenzije kazale superparamagnetno obnašanje.